

Fatigue in low-strength silica optical fibres

SHIGEKI SAKAGUCHI, YOSHINORI HIBINO

Ibaraki Electrical Communication Laboratory, Nippon Telegraph and Telephone Public Corporation, Tokai, Ibaraki 319-11, Japan

Fatigue behaviour was investigated for low-strength silica fibres on which macroscopic flaws were forcibly introduced by abrading. Crack growth in silica glass was also examined on the CT specimen. Stable crack growth parameters, obtained from the static and dynamic fatigue tests for abraded fibres, were determined to be about 40 which is equal to that obtained from the CT specimen, indicating that the crack growth process in abraded fibres is quite the same as in the CT specimen. This leads to the conclusion that, for the optical fibre, the allowable stress condition wherein no breaks occur is given on the basis of some basic fracture mechanics parameters obtained from the CT specimen.

1. Introduction

In an optical fibre, there are many kinds of flaws, which degrade mechanical strength, of various sizes along the longitudinal direction, randomly. A break in a long fibre due to fatigue fundamentally originates at a macroscopic flaw. The failure strength for the fibre is also dominated by this flaw. Thus, it is important to clarify the fatigue behaviour for a fibre containing macroscopic flaws to confirm high reliability.

The fatigue behaviour is mainly characterized by crack growth parameter n . The value of n for low-strength fibres which contain macroscopic flaws has not been sufficiently clarified, because only a few examinations have been made on low-strength fibres [1, 2], although many studies have been made on high-strength fibres which have no macroscopic flaws [3-5]. It is useful to compare the fatigue behaviour for low-strength fibres with crack propagation in a silica glass plate. On the other hand, it is very difficult to measure the flaw size directly on a fibre, because the flaw, even though it is a macroscopic one, is smaller than 10^{-3} mm. However, a proof test can offer an evaluation of the maximum flaw which remains in the fibre which has been proof-tested [6]. Therefore, when the fatigue behaviour for a macroscopic flaw is well understood and the maximum flaw is given by the proof test, long-term reliability for fibres can be assured.

In this report, the fatigue behaviour for low-strength fibres is studied and the allowable loading

condition for the macroscopic flaw not to begin to grow is discussed in order to assure high reliability for the fibre.

2. Experimental procedure

2.1. Sample

To examine the fatigue behaviour for low-strength fibres, an abraded silica fibre with silicone coating was drawn from a synthetic silica rod. The fibre was abraded by passing through a pulley, in whose slot no. 1500 emery paper had been adhered, prior to silicone coating, as shown in Fig. 1. The diameters of the fibre and silicone coatings are $125 \pm 1 \mu\text{m}$ and $\approx 450 \mu\text{m}$, respectively.

To examine the crack growth in silica glass, a WOL (wedge opening loading) type CT (compact tension) specimen was prepared. The configuration is shown in Fig. 2.

2.2. Fatigue testing

The abraded fibres were examined by means of static and dynamic loading testings. In the static test, a constant tensile load was applied to the fibre, because the flaws are randomly distributed on the fibre surface along circular and longitudinal directions. Static loading was applied to the fibre at 200 mm gage length in distilled water at 20°C .

Dynamic test were performed at 0.125 to $16.7 \text{ GPa min}^{-1}$ loading rate and 200 mm gage length in air at 20°C and 60% r.h., using a conventional tensile testing machine. Twenty replicate measurements were made at each loading rate.

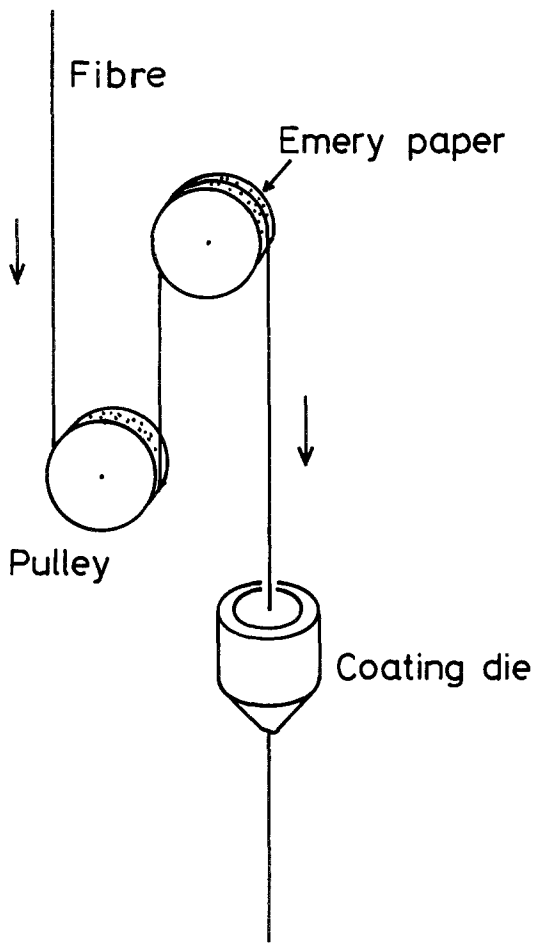


Figure 1 Schematic representation for abraded fibre drawing.

The crack growth in the CT specimen was directly measured under slow strain rate dynamic loading at $0.0005 \text{ mm min}^{-1}$. The time dependent change in crack length was measured by using an ITV incorporating a VTR, as described in [7].

3. Results

3.1. Fatigue in abraded fibres

Time-to-failure measured on abraded fibres is shown plotted against the applied stress in Fig. 3. Scattering ranges for the times to failure (solid circles represent average values) are shown in the figure.

An almost linear relationship is obtained between log time-to-failure, t_f , and log applied stress, σ_a , expressed by

$$\ln t_f = -n \ln \sigma_a + \ln S \quad (1)$$

where n and S are constants dependent on the

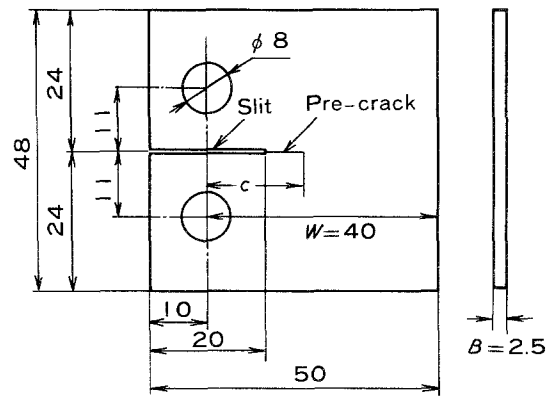


Figure 2 CT (compact tension) specimen configuration.

environment. The fatigue behaviour is mainly characterized by the parameter n , which refers to the crack growth parameter. The value of n is determined to be 35.6 from the present experiment. This is almost the same as the value reported previously [1].

Fig. 4 shows the dynamic test results, tensile strength change against the loading rate, for abraded fibres. Scattering ranges of the strengths are shown in the figure, indicating the average values by solid circles.

The strength shows an increase with an increase in the loading rate, described by

$$(n + 1) \ln \sigma_f = \ln \dot{\sigma} + \ln D \quad (2)$$

where D is a constant. From the data shown in Fig. 4, the value of n is obtained as 42.6, which is almost the same as that obtained from the static test. The parameter, n , is considered to be a function of temperature only for silicone-coated fibres [4]. Although dynamic tests were carried out in air, it is valid to compare the value of n with that obtained in water, because the temperature is the same.

It is noted that the values of n obtained by both static and dynamic tests for abraded fibres are around 40, which is twice the value, 20, obtained for high-strength fibres containing no macroscopic flaws.

3.2. Crack growth in CT specimen

Fig. 5 shows the time dependent change in crack length observed in a silica glass CT specimen under slow strain rate dynamic loading at $0.0005 \text{ mm min}^{-1}$. Remarkable stable crack growth was observed even under dynamic loading. In this case, the crack grows stably for more than 4 mm.

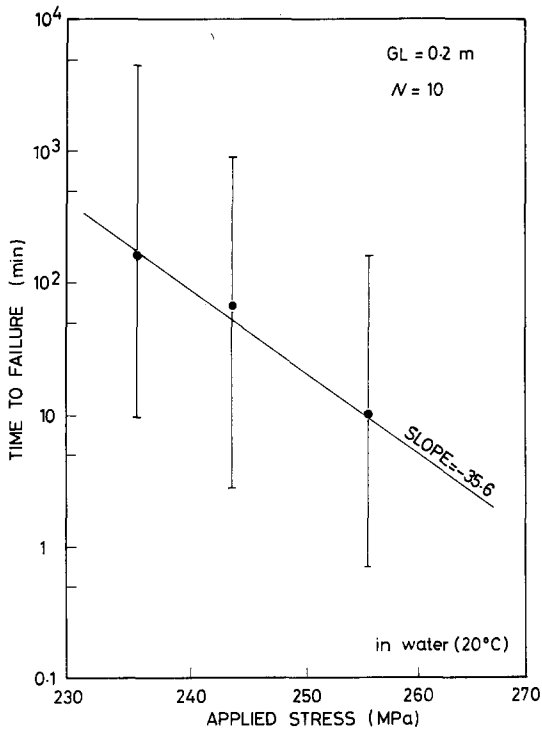


Figure 3 Time-to-failure for abraded fibres against applied stress in distilled water at 20°C.

The crack growth rate dc/dt , calculated from the growth curve shown in Fig. 5 is plotted against the stress intensity factor, K , in Fig. 6. A linear relationship is obtained between log growth rate, dc/dt , and log stress intensity factor, K , which is described by

$$dc/dt = AK^n \quad (3)$$

where A is a constant. The values of n and log A

obtained from the present data are listed in Table I with those obtained from the static test [8]. These values are very close to each other independent from the loading method used, indicating that the same process under static loading occurs in the crack growth under dynamic loading.

The growth parameter, n , of about 40 is also obtained from the crack growth data for the CT specimen, as well as from abraded fibres. This fact indicates that, in a low-strength fibre, the value of n must be taken as ≈ 40 for the growth process originated at a macroscopic flaw, which is considered to be a continuity because of its very large size compared with an interatomic distance for the Si-O bond.

On the other hand, the value of n , 40, for abraded fibres is almost twice that obtained from high-strength fibres. A break in a high-strength fibre originates at a surface microscopic defect whose size is thought to be of the order of the interatomic distance [4]. When an external stress is applied to the defect, it grows to macroscopic critical size, followed by spontaneous fracture. It seems that the early stage in the growth process for the microscopic defect cannot be regarded as a continuity, which is described on the basis of the fracture mechanics concept. Thus, two stages for the microscopic defect growth process are considered, the early stage from microscopic to macroscopic size, and the growth process as a continuity itself. Since, for calculating the n value for high-strength fibres, these stages are treated at the same time, a difference in the value of n might appear for high and low-strength fibres.

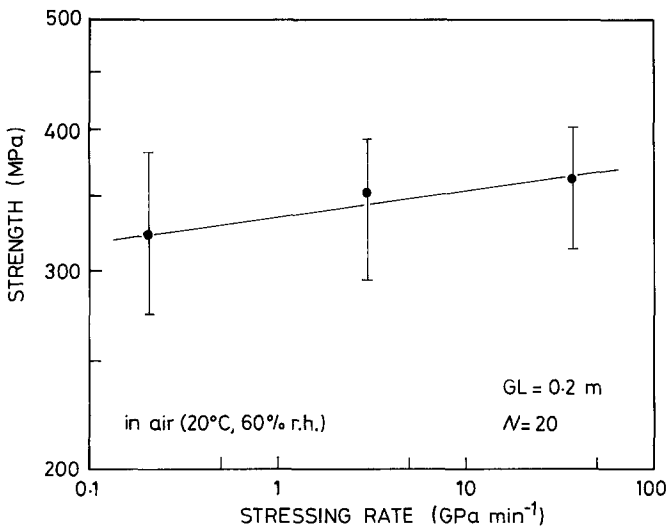


Figure 4 Tensile strengths for abraded fibres against loading rate in air at 20°C and 60% r.h.

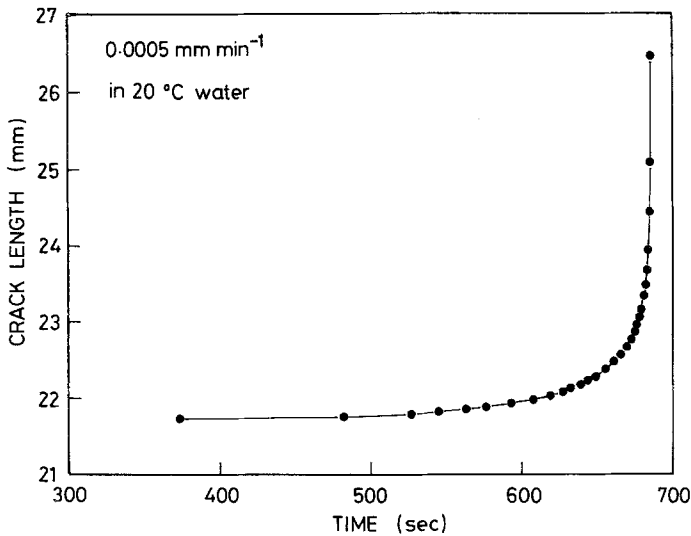


Figure 5 Time dependent change in crack length, obtained from CT specimen loaded at a crosshead speed of $0.0005 \text{ mm min}^{-1}$ in distilled water at 20° C .

4. Allowable stress condition

It is very important to clarify the minimum strength for a long fibre in order to confirm its reliability. Proof testing aims to guarantee the minimum strength level for a fibre, which has passed the proof test, corresponding to the proof stress. The relationship between the proof stress and the minimum strength was clarified experimentally [6]. When the unloading rate at the final

stage in the proof test cycle is fast enough that crack growth during unloading can be neglected, the maximum size for a flaw which remains in the fibre after proof testing is given by the following equation,

$$K_{\text{IC}} = \sigma_p Y(c_p)^{1/2} \quad (4)$$

where K_{IC} is the fracture toughness, σ_p is the proof stress, Y is the geometric parameter ($= 1.24$ for a halfpenny shaped crack existing on the fibre surface), and c_p is the maximum crack size.

On the other hand, it is well known that, when the stress condition is lower than the critical stress intensity for stress corrosion cracking K_{ISCC} , no stable crack growth occurs. In addition, it was clarified that the fatigue behaviour for abraded fibres having macroscopic flaws is quite the same as for the CT specimen from the result of the present experiment. This indicates that a lower limit for crack growth in abraded fibre also exists, i.e. the critical condition is given by K_{ISCC} , which cannot be measured directly on the abraded fibre. Based on this assumption, allowable applied stress σ_a , at which no growth will occur for the maximum crack c_p , which is guaranteed by the proof test is given by

$$K_{\text{ISCC}} = \sigma_a Y(c_p)^{1/2} \quad (5)$$

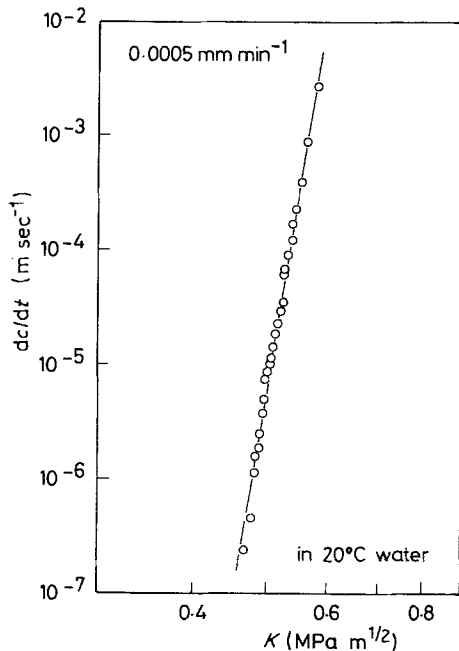


Figure 6 Crack growth rate, dc/dt , in CT specimen, calculated from the data shown in Fig. 5, against stress intensity factor, K .

TABLE I Summary of n and $\log A$ values obtained from the CT specimen

Loading	n	$\log A$
$0.0005 \text{ mm min}^{-1}$	42.0	-235
Constant stress [8]	40.5	-237

From Equations 4 and 5, the allowable stress is expressed by

$$\sigma_a = \sigma_p K_{ISCC} / K_{IC} \quad (6)$$

In other words, when the stress condition is given from considerations of cable laying process, cable structure, etc., the required proof stress can be determined from Equation 6, in order that no break in the fibre would occur.

For example, in water, the K_{ISCC} value is evaluated as $0.37 \text{ MPa m}^{1/2}$ [8], to which a similar value is estimated from the present experiment, while the K_{IC} is $0.78 \text{ MPa m}^{1/2}$ [9]. Thus, the fibre must pass the proof test at the stress given by

$$\sigma_p = 2.1 \sigma_a$$

Fig. 7 shows the required proof stress plotted against the applied stress for silica fibres in water.

The above discussion gives the non-break conditions for optical fibres, using some basic fracture mechanics parameters, which were obtained using a CT specimen. This was confirmed by the present result, wherein the crack growth process for macroscopic flaws was the same as for the CT specimen. The slow strain rate dynamic loading test was one of the conventional methods used in order to examine the growth process in various environments.

5. Conclusion

An investigation on fatigue behaviour for low-strength fibres was made in order to assure their long-term reliability. Furthermore, the allowable stress conditions, wherein fatigue failure would not occur, was discussed. The results are as follow:

1. For abraded fibres, on which macroscopic flaws are forcibly introduced, the values of crack growth parameters were determined from static and dynamic loading tests to be 35.6 and 42.6, respectively.

2. From the slow strain rate dynamic text on the CT specimen, the value of n was obtained as 42.0 which is almost equal to the values for abraded fibres, indicating that the growth process in both abraded fibres and the CT specimen is the same.

3. It is proposed that the critical loading conditions, under which silica optical fibre would not

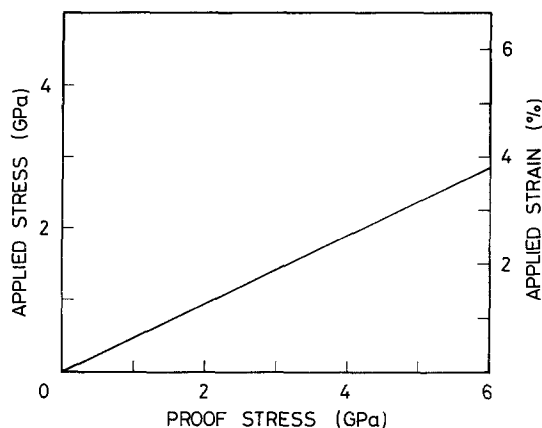


Figure 7 Relationship between allowable stress and required proof stress.

break due to fatigue, are given by using some basic fracture mechanics parameters obtained from the CT specimen.

Acknowledgements

The authors would like to thank N. Inagaki, S. Yamakawa, Y. Tajima, and K. Chida for encouragement and are indebted to M. Nakahara for useful discussions.

References

1. S. T. GLATI, J. D. HELFINSTINE, B. JUSTICE, J. S. McCARTNEY and M. A. RUNYAN, *Amer. Ceram. Soc. Bull.* **58** (1979) 1115.
2. F. A. DONAGHY and D. R. NICOL, *J. Amer. Ceram. Soc.* **66** (1983) 601.
3. D. KALISH and B. K. TARIYAL, *ibid.* **61** (1978) 518.
4. S. SAKAGUCHI and T. KIMURA, *ibid.* **64** (1981) 259.
5. H. C. CHANDAN and D. KALISH, *ibid.* **65** (1982) 171.
6. S. SAKAGUCHI and M. NAKAHARA, *ibid.* **66** (1983) C-46.
7. Y. HIBINO, S. SAKAGUCHI and Y. TAJIMA, *J. Mater. Sci. Lett.* **2** (1983) 388.
8. S. SAHAGUCHI, S. SAWAKI, Y. ABE and T. KAWASAKI, *J. Mater. Sci.* **17** (1982) 2878.
9. S. M. WIEDERHORN, *J. Amer. Ceram. Soc.* **52** (1969) 99.

Received 28 December 1983
and accepted 16 January 1984